Proceedings of the VIII Serbian-Bulgarian Astronomical Conference (VIII SBAC)
Leskovac, Serbia, May 8-12, 2012,
Editors: M. S. Dimitrijević and M. K. Tsvetkov
Publ. Astron. Soc. "Rudjer Bošković" No 12, 2013, 143-152

KINEMATICS OF A LOOP-LIKE ERUPTIVE PROMINENCE AS OBSERVED BY AIA/SDO

M. DECHEV[1] , K. KOLEVA[1], M. S. MADJARSKA[2], P. DUCHLEV[1], J.-C. VIAL[3], E. BUCHLIN[3]

[1]*Institute of Astronomy and National Astronomical Observatory, BAS,*
[2]*Armagh Observatory, College Hill, Armagh, N. Ireland*
[3]*Univ Paris-Sud, Institut d'Astrophysique Spatiale, Orsay, France*

Abstract. We examined the kinematic and helicity pattern, as well as the morphological and geometrical evolution of an EP on 2010 March 30. We used the He II 304 A AIA/SDO and EUVI/STEREO B observations. The unique combination of high-resolution limb observations of the EP in AIA and a central meridian position in EUVI permitted a view from significantly different perspectives and detailed analysis of the prominence eruption. The eruption process consists of prominence activation, acceleration, and a phase of constant velocity. The prominence body was composed of left-hand twisted threads around the main prominence axis. The twist during the eruption was estimated at 3 turns (6 pi). The prominence reformed in the same place two days after its eruption. The same sign of the prominence body twist and writhe, as well as the amount of twisting above the critical value of 2pi after the activation phase indicate that the conditions for kink instability were present. The fact that the erupted filament re-formed at the same place two days after the eruption implies a confined type of eruption.

1. INTRODUCTION

Prominence eruptions are large-scale eruptive phenomena, which occur in the low solar atmosphere. Eruptive prominences (EP), in contrast to active ones, could be defined as prominences in which all or some of the prominence material appears to escape the solar gravitational field (Gilbert et al., 2000). Gilbert et al. (2007) summarize three types of prominence eruptions: a full eruption, when all of the material is expelled; a partial, when only a part of the mass erupts; or a failed eruption, if the material resettles or falls back to the surface. The observations show that prominence/filament activations include a wide range of eruptive-like dynamic activity, from the full eruption (Plunkett et al., 2000) through partial eruption (Zhou et al. 2006; Liu et al., 2008) to failed eruption. Several studies

(Sterling & Moore, 2004 a, b) have unveiled a common pattern of prominence (filament) eruptions: an initial slow-rise phase (with very small acceleration), during which the filament gradually ascends, followed by a sharp change to a fast-rise phase of fast acceleration. The eruption onset has been defined as the transition between these two phases. There are three scenarios for a prominence rising after its fast rise phase: 1) an EP can continue to raise with acceleration, 2) an EP fast rise can be followed by a constant velocity phase, or 3) a constant velocity phase of a EP can be followed by a deceleration phase (Vrsnak, 1998).

The slow rise motion of an EP is accompanied by a gradual morphological evolution from an initially intricate structure into an apparently toroidal shape, exposing sometimes a twisted pattern, that is most often prominent in the legs of the prominence (Vrsnak et al., 1991). EPs very often develop a clearly helical axis shape in the course of the eruption, which is the characteristic signature of a MHD kink instability (KI) of a twisted magnetic flux rope (MFR) (Rust & LaBonte, 2005). A MFR becomes kink-unstable if the twist, a measure of the number of windings of the field lines about the rope axis, exceeds a critical value of 2π (Hood and Priest,1981). The axis of an MFR then undergoes writhing (kinking) motions and part of the twist of the field is transformed into helical writhe of the axis, since the magnetic helicity is essentially conserved (Rust & LaBonte, 2005). The conservation of helicity in ideal MHD (Berger, 1984) requires the resulting writhe to be of the same sign as the transformed twist (Green et al., 2007). The kink instability has long been investigated as a possible triggering mechanism for solar eruptive phenomena, especially in flux rope models (Liu and Alexander, 2009).

2. OBSERVATIONAL MATERIAL

The prominence eruption was observed at the North-East solar limb between 17:30 UT and 19:30 UT on 2010 March 30. The EP was located at mean heliographic co-ordinates N22.63°; E78.80° and centered mean position angle 66°.

The analyzed images were taken with 1 min cadence in the He II 304 Å pass-band of AIA/SDO (Lemen et al., 2011). The AIA instrument consists of seven Extreme Ultra-Violet (EUV) and three Ultra-Violet (UV) channels which provide an unprecedented view of the solar corona with an average cadence of about 12s. The AIA image field-of-view reaches 1.3 solar radii with a spatial resolution of about 1.5 arcsec.

First, we selected a partial field-of-view (FOV) from the AIA He II 304 Å images. We used level 1 reduced data, i.e. the dark current removed and flat-field correction applied. We extracted 700 x 1000 pixels^2 cut-outs from the full FOV images. The images were further stabilized for the satellite movements by applying intensity cross-correlation analysis. For the purpose of our analysis we defined the visible limb from the He II 304 Å images.

We also analyzed observations from the Extreme Ultraviolet Imager (EUVI) aboard STEREO Behind (B) spacecraft. EUVI has a field-of-view of 1.7 $R_{\odot}$ and

observes in four spectral channels that cover the 0.1 to 20 MK temperature range (Wuelser et al., 2004). The EUVI detector has pixel size of 1.6 arcsec.

In the present study we used EUVI images in the He II 304 Å channel with an average cadence of 10 minutes.

3. MORPHOLOGY AND HELICITY EVOLUTION

The prominence eruption evolved as a height expanding twisted loop with both legs anchored in the chromosphere of a plage area.

The prominence can be observed in H-alpha before the activation at 17:19 UT (Fig.1) as a few bright clouds above the limb with no distinguishable fine structure.

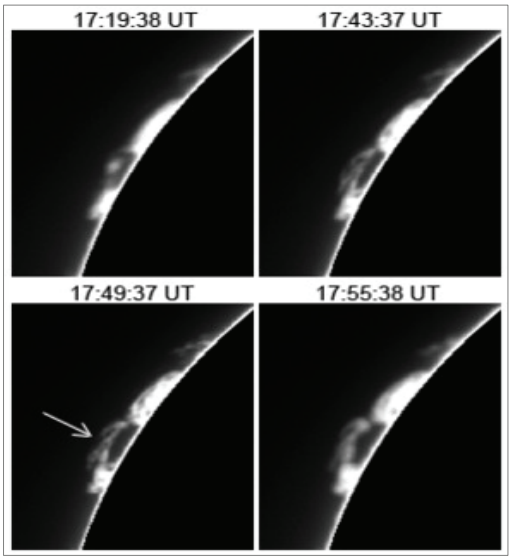

Figure 1: Mauna Loa H-alpha images before and during the start of the prominence activation. The arrow points at the region revealing twisted structure.

The first signature of a twisted prominence fine structure appears at 17:49 UT in the AIA He II 304 Å image (Fig.2). From part of the prominence where the fine structure is visible, we could estimate a 2π twist, i. e. one turn of the prominence rope around its main axis. This time coincides with the beginning of the prominence slow rise during the activation phase. The total twist was estimated to be of about 6π (3 turns) of the eruptive prominence body.

After 18:25 UT the eruption can also be followed on the EUVI/STEREO image differences shown in Fig. 3. Here, thanks to the different view point we could see

that the filament upper body underwent a left-hand writhe, which increase with time, reaching π/2 at 19:26 UT.

The helical twist of the prominence and its evolution in time can be clearly seen in AIA He II 304 Å images after 18:20 UT. During the prominence rise the twist transfers from the lower (legs) to the upper prominence body causing the prominence to evolve from a loop-shaped into a ribbon-like structure. From the EUVI B difference images (Fig. 3), we established the footpoint location in order to determine the type of twist and writhe, and their evolution in time. Based on the magnetic field polarity configuration obtained from the magnetograms, the H-alpha images and the prominence drawings (Fig. 7), we could determine in which magnetic polarity the southern and the northern legs of the prominence were located. We determined that the prominence underwent a left-hand writhe as a result of counter-clockwise rotation with respect to the two polarity fluxes.

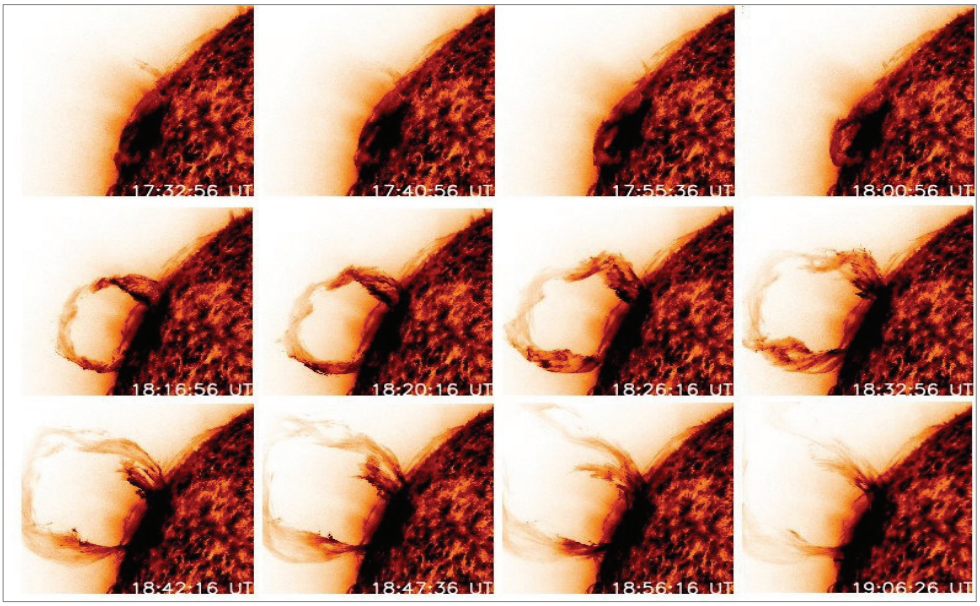

Figure 2: He II 304 Å images (in reversed colour table) showing the morphology and, in particular, the helicity evolution of the erupting prominence.

Figure 3: Running difference images from EUVI B in the He II 304 Å channel.

4. KINEMATICS

The prominence height was determined as the height of the main axis of the prominence above the visible limb as observed in the He II 304 Å channel of the AIA/SDO images (Fig. 4). The time evolution of the height reveals three distinctive phases of the prominence eruption: prominence activation, an eruption with acceleration, and an eruption with a constant velocity. The height-time diagram of the prominence eruption is presented in Fig. 5. From the first and second derivatives of the polynomial fit of the height-time curve, we defined the speed and the acceleration of the prominence eruption. The prominence activation is defined as the time period of a slow rise of the loop system with a velocity of 10 km/s. The activation is already in progress at the beginning of the AIA observations around 17:33 UT. Until 18:00 UT the height of the prominence

changed from 18 Mm to 34 Mm. The eruption onset was registered at 18:00 UT and it was determined from the AIA images as a sudden increase of the prominence height. It lasted until around 18:12 UT (Fig. 5). During this phase the prominence height changed from 34 Mm to 121 Mm and the speed of the prominence rise increased from 15 kms^{-1} to a maximum of 166 kms^{-1} with an acceleration from 46 to 430 ms^{-2}. The constant velocity phase was measured until 18:44UT. After this time the top of the looped prominence is outside the AIA field-of-view.

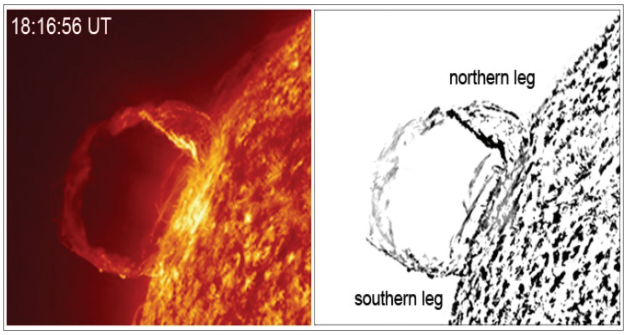

Figure 4: The eruptive prominence on 2010 March 30 observed in the 304 Å AIA/SDO channel at 18:17 UT (left**)** and its corresponding edge-enhanced image (right).

We used also, as an additional geometrical parameter, the diameter at the summit **D** of the main prominence MFR. Its dependence as a function of time is given in Fig.6. The time profile of **D** clearly shows two phases in its behavior: slow decrease during a 51-minute time interval and strong increase during an 8-minute time interval. The comparison of the time profiles of **D** and the EP height in Fig.6 shows that the decrease of **D** covers the activation, acceleration, and half of the constant velocity phase of the EP.

The kinematics of the different phases of the eruptive process is summarized in Table 1.

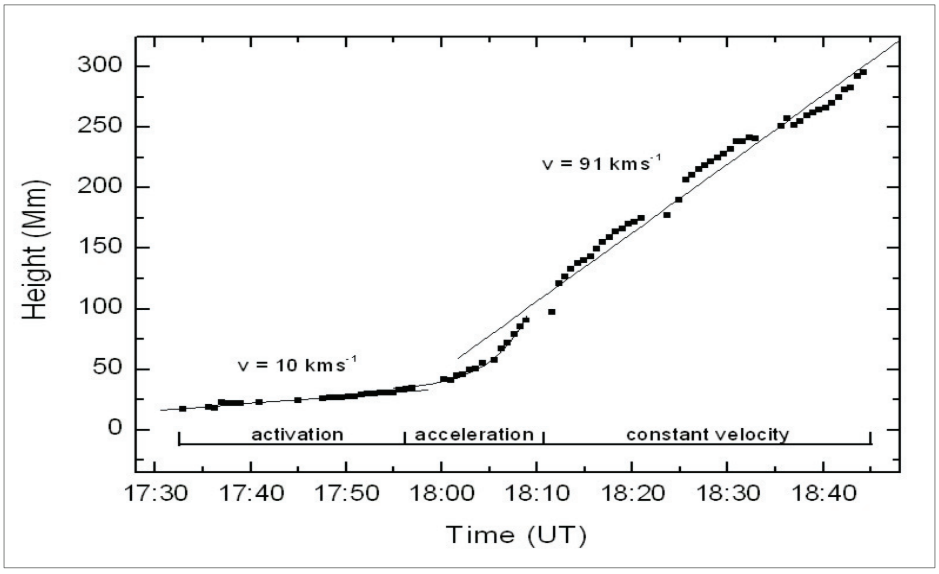

Figure 5: Height-time profile of the prominence eruption for the three phases of the EP evolution: the activation, the acceleration, and the constant velocity.

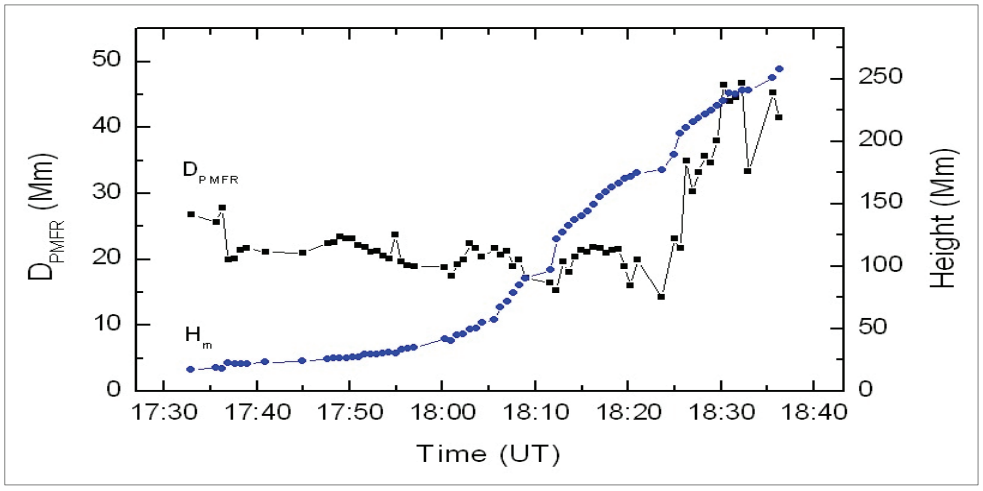

Figure 6: Time profile of the diameter **D** of the main prominence magnetic flux rope (PMFR) at the EP summit. The time profile of the height of the axis of main PMFR is shown, too.

Table.1: Kinematics of the eruptive prominence derived from the AIA images.

Phase	Time (UT)	Height (Mm)	Velocity (km s^{-1})	Acceleration (m s^{-2})
Activation	17:33 – 18:00	18 - 34	10	0
Acceleration	18:00 – 18:12	34 - 121	15 – 166	46 – 430
Constant velocity	18:12 – 18:44	121 – 295	91	0

5. REFORMATION

The prominence reformed in the same place two days after its eruption. In Fig. 7 the re-formation of the filament is presented from March 31 to April 2. On March 31, one day after its eruption, the filament can be traced above and below the plage area on the Coimbra Solar Observatory H-alpha (Fig.7a). The magnetic field of the plage area associated with the reforming filament can be seen in Fig.7b. Figs.7 c, d, e and f show H-alpha images and drawings of the area from the Pulkovo Observatory, confirming the reformation of the filament. However, we can notice that the H-alpha filament is rather faint. We searched for its reformation in the EUV lines of EUVI B, but even in He II it was not possible to detect it. One can conclude that even if the eruption failed, the material was not totally recovered at the low temperature typical of a filament.

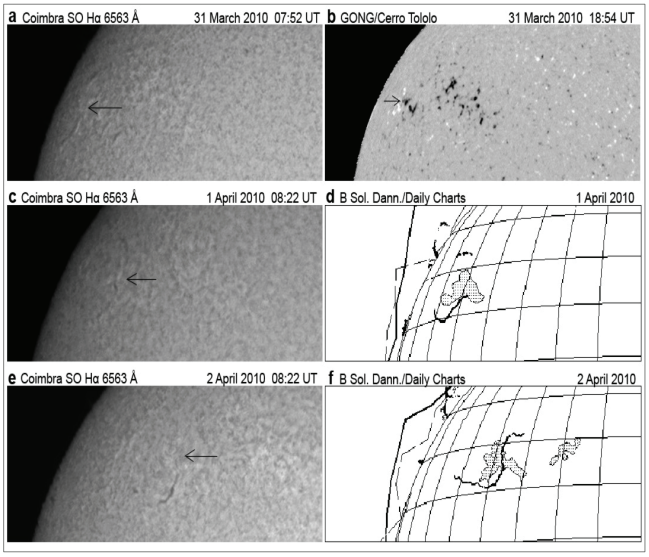

Figure 7: The prominence reformation as seen on the disk as a filament traced in Coimbra Solar Observatory H-alpha images (**a, c, e**), a GONG magnetogram (**b**), and daily drawings of the Sun from the electronic Bulletin "Solnechnye Dannye" of Pulkovo Observatory (**d** and **f**).

6. RESULTS

We examined the kinematic and helicity pattern together with the morphological and geometrical evolution of an EP, based on He II 304Å AIA/SDO and EUVI/STEREO B observations. The unique combination of high-resolution limb observations of the EP in AIA and a central meridian position in EUVI B permitted a detailed analysis of the prominence eruption on 2010 March 30. The obtained results can be summarized as follow:

- The EP appeared as a helically twisted MFR with fixed foot-points. The prominence's body was composed of left-hand twisted threads around the main prominence axis. The twist during the eruption was estimated to be 6π (3 turns).
- The EP twist progressively converted into a left-hand writhe that is clearly traced in the EUVI/STEREO B images.
- The prominence contracted to its primary location after reaching a maximum height of 526 Mm. The prominence/filament partially reformed, suggesting that either part of the material has drained into the photosphere or that not all of the prominence material returned to its primary temperature.

Acknowledgments

One of the authors (M. D.) is supported by a grant of the Bulgarian National Science Foundation, Ministry of Education and Science, under number DO-02-275.

References

Berger, M. A.: 1984, *Geophysical and Astrophysical Fluid Dynamics*, **30**, 79.
Gilbert, H. R., Alexander, D., Liu, R.: 2007, *Sol. Phys*., **245**, 287.
Gilbert, H. R., Holzer, T. E., Burkepile, J. T., Hundhausen, A. J.: 2000, *ApJ*, **537**, 503.
Green, L. M., Kliem, B., Torok, T., van Driel-Gesztelyi, L., Attrill, G. D. R.: 2007, *Sol. Phys*., **246**, 365.
Hood, A. W., Priest, E. R.: 1981, *Geophysical and Astrophysical, Fluid Dynamics*, **17**, 297.
Lemen, J. R., Title, A. M., Akin, D. J., et al.: 2011, *Sol. Phys*., 172.
Liu, R., Alexander, D.: 2009, *ApJ*, **697**, 999.
Liu, R., Gilbert, H. R., Alexander, D., Su, Y.: 2008, *ApJ*, **680**, 1508.
Plunkett, S. P., Vourlidas, A., Simberova, S., et al.: 2000, *Sol. Phys*., **194**, 371.
Rust, D. M., LaBonte, B. J.:2005, *ApJ*, **622**, L69.
Sterling, A. C., Moore, R. L.: 2004a, *ApJ*, **602**, 1024.
Sterling, A. C., Moore, R. L.: 2004b, *ApJ*, **613**, 1221.
Vršnak, B.:1998, In: IAU Colloq. 167: *New Perspectives on Solar Prominences*, Eds.. D. F. Webb, B. Schmieder, D. M. Rust, *Astronomical Society of the Pacific Conference Series*, **150**, 302.
Vršnak, B., Ruždjak, V., Rompolt, B.:1991, *Sol. Phys*., **136**, 151.

Wuelser, J., Lemen, J. R., Tarbell, T. D., et al.: 2004, In: *Society of Photo-Optical Instrumentation Engineers (SPIE) Conference Series*, Eds.S. Fineschi, M. A. Gummin, **5171**, 111.

Zhou, G. P., Wang, J. X., Zhang, J., et al.: 2006, *ApJ,* **651**, 1238.